



MISSOURI
S&T

CENTER FOR TRANSPORTATION INFRASTRUCTURE AND SAFETY



Testing and Assessment of Portable Seismic Property Analyzer

by



Neil Anderson
Mengxing Li



**A National University Transportation Center
at Missouri University of Science and Technology**



**NUTC
R297**

Disclaimer

The contents of this report reflect the views of the author(s), who are responsible for the facts and the accuracy of information presented herein. This document is disseminated under the sponsorship of the Department of Transportation, University Transportation Centers Program and the Center for Transportation Infrastructure and Safety NUTC program at the Missouri University of Science and Technology, in the interest of information exchange. The U.S. Government and Center for Transportation Infrastructure and Safety assumes no liability for the contents or use thereof.

Technical Report Documentation Page

1. Report No. NUTC R297	2. Government Accession No.	3. Recipient's Catalog No.	
4. Title and Subtitle Testing and Assessment of Portable Seismic Property Analyzer		5. Report Date February 2014	
		6. Performing Organization Code	
7. Author/s Neil Anderson		8. Performing Organization Report No. Project # 00038172	
9. Performing Organization Name and Address Center for Transportation Infrastructure and Safety/NUTC program Missouri University of Science and Technology 220 Engineering Research Lab Rolla, MO 65409		10. Work Unit No. (TRAIS)	
		11. Contract or Grant No. DTRT06-G-0014	
12. Sponsoring Organization Name and Address U.S. Department of Transportation Research and Innovative Technology Administration 1200 New Jersey Avenue, SE Washington, DC 20590		13. Type of Report and Period Covered Final	
		14. Sponsoring Agency Code	
15. Supplementary Notes			
16. Abstract Investigator will thoroughly test and assess the Portable Seismic Property Analyzer (PSPA), a hand-held device that focuses on pavement layer properties. The device can be utilized on both rigid and flexible pavements. When used on rigid pavements, the PSPA can provide information with respect to the quality and thickness of concrete, the existence and/or the location of voids or delamination within concrete, and the existence of voids or the loss of support underneath the slab. For flexible pavements, the PSPA provides information about the quality of the asphaltic-concrete layer.			
17. Key Words Seismic, pavements, concrete, asphalt, defects	18. Distribution Statement No restrictions. This document is available to the public through the National Technical Information Service, Springfield, Virginia 22161.		
19. Security Classification (of this report) unclassified	20. Security Classification (of this page) unclassified	21. No. Of Pages 36	22. Price

Testing and Assessment of Portable Seismic Property Analyzer

**Neil Anderson
Mengxing Li
Missouri Science & Technology**

PROJECT SUMMARY

The condition of the transportation network in the United States is deteriorating and requires enormous financial and human resources for its maintenance and mitigation. According to the National Bridge Inventory [39], about 25.4% of 600,000 bridges in the United States are structurally deficient or obsolete. The health monitoring of concrete bridge decks and pavements is critical for its maintenance and rehabilitation. Rapid, non-destructive, and accurate condition assessment and performance monitoring of bridge decks and pavements will significantly reduce the cost and human resource for its maintenance and rehabilitation.

The dominant current practice used by the state departments of transportation (DOTs) for inspection of concrete bridge decks and pavements has been chain dragging and hammer

sounding. They can be described as nondestructive and relatively rapid. However, the accuracy of chain dragging and hammer sounding are significantly compromised by the fact that they can be used only to identify delamination at stages in which the deterioration has already progressed to such an extent that major rehabilitation measures are needed. Furthermore, these traditional inspection methods cannot provide important monitoring parameters directly related to the health condition of bridge decks and pavements, such as the strength of the concrete and the depth of the delamination. The modern nondestructive techniques have been widely used as routine inspection methods for bridge deck and pavement evaluation in recent years. Ground penetrating radar (GPR) and seismic testing methods are two popular modern nondestructive techniques and their advantages are significant compared with traditional inspection methods.

Ground penetrating radar has been successfully used for bridge deck and pavement evaluation over two decades. The principle of the method is using electromagnetic waves to locate objects buried inside the structure and to produce contour maps for subsurface features, such as reinforcement steels and wire meshes [18]. Ground penetrating radar method has been demonstrated successfully used for corrosion induced delamination detection with rapid acquisition speed by many transportation department and industry agencies. However, the information about the mechanical properties (e.g., strength, modulus) of materials cannot be obtained by GPR survey. Also, the definitive information about the presence of corrosion, corrosion rates or reinforcement steel section loss also cannot be provided by GPR survey.

In recent years, the portable seismic property analyzer (PSPA) which integrated two seismic testing methods: impact-echo (IE) and ultrasonic surface wave (USW), has been successfully used to detect common defects in concrete bridge decks and pavements as one of the modern nondestructive techniques [20], [21], [33]. The benefits of these methods are significant compared with those traditional inspection methods from several aspects: First of all, the elastic modulus of materials can be determined in the field rapidly and precisely, no other method can provide such a capability. Furthermore, it has been demonstrated that PSPA can detect and assess delamination at various deterioration stages, especially in the early stage of deteriorations [35], [36]. However, PSPA has not been used extensively by the state department of transportation agencies due to several reasons:

- First of all, the PSPA instrument is a point loading system, data acquisition time for each point is approximately 30 seconds. Therefore, the data acquisition procedure can be very slow and intensive labor is needed for the large scale testing task. Furthermore, the PSPA instrument is highly sensitive to the surface condition of the test area. Cracking or rough surface can significantly affect the quality of PSPA data. The improper operations of the instrument such as poor coupling to the testing surface can also affect the quality of PSPA data.
- Second, the PSPA data processing and interpretation is not always straightforward and simple. The automatic output test results are not always reasonable and need to be inspected carefully. The high level ambient noise induced by the complex internal structure of bridge deck or pavement, such as reinforcement steel and

construction joint can significant effect the impact-echo data interpretation. Furthermore, the overestimated P-wave velocity derived from the surface wave velocity can also affect the accuracy of impact-echo data calculation.

- Last, the general protocol for PSPA data acquisition, processing and interpretation has not been established in order to guidance people using PSPA effectively and properly for the rapid condition assessment of concrete bridge decks and pavements.

The first task of this study is to evaluate the capabilities of PSPA for identifying and characterizing common defects in concrete bridge decks and pavements. The second task of this study is to identify current problems and misleadings found during the procedure of PSPA data acquisition, processing and interpretation. Improving and developing the current PSPA data processing and interpretation methods and makes it more accurate and easy to use. The last task of this study is to establish a general protocol for PSPA data acquisition, processing and interpretation to help and guidance people using PSPA technique effectively and properly for the rapid condition assessment of concrete bridge decks and pavements in the future. The following specific steps have been conducted in this study in order to meet the requirement of the project:

- The locations of reinforcement steels have been marked using GPR method before conducted PSPA field test. For each PSPA test point, the PSPA instrument has been placed avoid overlaid on the top of reinforcement steels during the field tests of bridge decks evaluation in order to minimum the effect of ambient noise to impact-echo data interpretation.
- The comparison test results of PSPA, Lidar and GPR data verified by the borehole control and laboratory testing have been demonstrated in this study in order to evaluate the utility of PSPA for bridge deck or pavement deterioration detection.
- The assumed uniform P-wave velocity has been used in impact-echo data analysis instead of the overestimated P-wave velocity derived from the surface wave velocity in this study. The manual analysis of impact-echo data has been demonstrated more accurate and efficient than automatic analysis results by comparing with Lidar data.
- The uniform scale of modulus elasticity for concrete bridge decks and pavements evaluation has been generated and verified by Lidar, borehole and laboratory test results.
- The first frequency peak in impact-echo amplitude spectra has been identified as the reflection from the bottom of the deck instead of the most strong reflection frequency (return frequency) used for thickness calculation. The manual analysis of impact-echo data has been demonstrated more accurate and efficient than automatic analysis results by comparing with Lidar.

1. INTRODUCTION

1.1 THE BASIC THEORY OF PSPA

The portable seismic property analyzer (PSPA), shown in Figure 01, is an integrated ultrasonic seismic devices that measurement the change of elastic modulus and the thickness of bridge deck or pavement surface layers [20]. The PSPA is based on the nondestructive device developed by Dr. Baker [38] and consists of a source and two transducers packaged into a portable system for performing seismic tests in the field [36]. The device is connected to a laptop computer through a cable that carries commands to the PSPA and stores the signals collected by the transducers. The source package is also equipped with a transducer for consistency in triggering and for some advanced analysis of the signals [35].

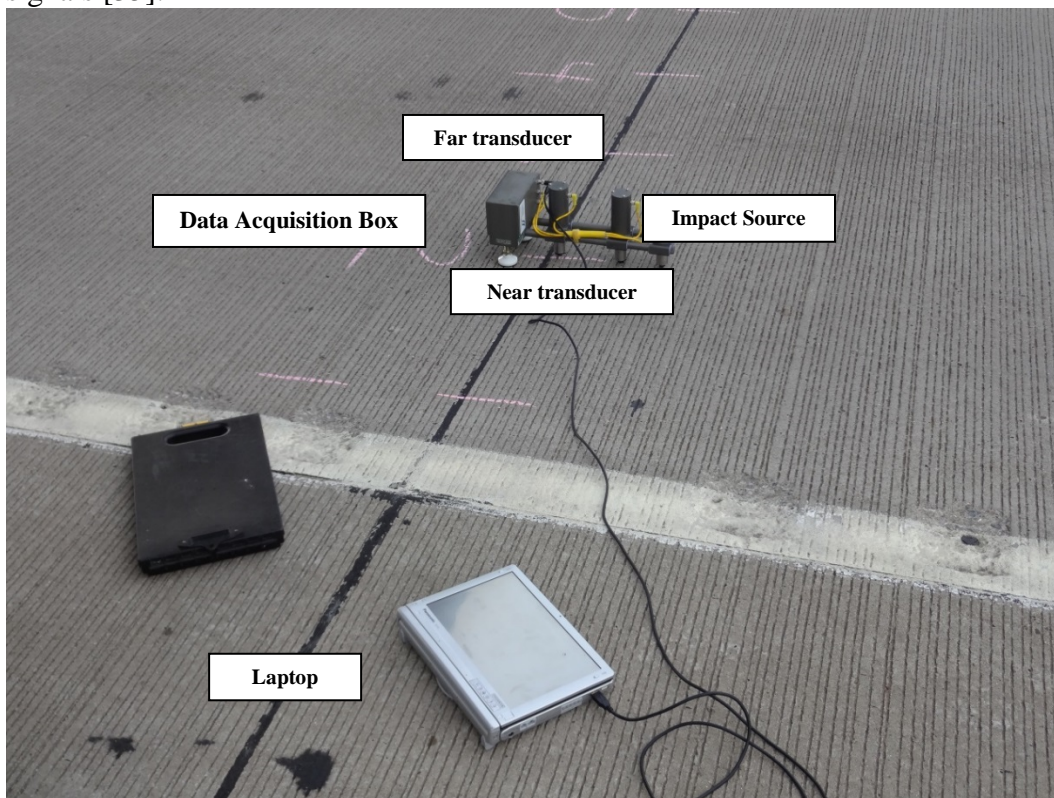


Figure 01: The Composition of Portable Seismic Property Analyzer (PSPA).

The principle of the PSPA is based on generating and detecting stress waves in a medium [35]. The PSPA data processing and interpretation is based on the ultrasonic surface wave (USW) and impact-echo (IE) methods. The basic theory for each method is briefly described in the following sections.

1.1.1 Ultrasonic Surface Wave

The ultrasonic surface wave method is used to determine the elastic modulus of the material. The most dominant waves generated and detected by the device are surface waves since it's contain about two-thirds of the seismic energy. At wavelengths less than

or equal to the thickness of the uppermost layers, the velocity of propagation is independent of wavelength [35]. Consequently, if the properties of the uppermost layer are summed to be uniform, the elastic modulus of the upper layer, E_{field} , can be determined simply by generating high-frequency (short wavelength) waves:

$$E_{\text{field}} = 2\rho[(1.13-0.16\nu)V_R]^2(1+\nu)$$

Where

V_R = velocity of surface waves,

ρ = mass density, and

ν = Poisson's ratio.

The variability of test results with the PSPA on Portland cement concrete is less than 3% without moving the device and around 7% when the device is moved in a small area [38]. The general procedure of evaluation the elastic modulus of the material through the ultrasonic surface wave method has been shown in Figure 02.

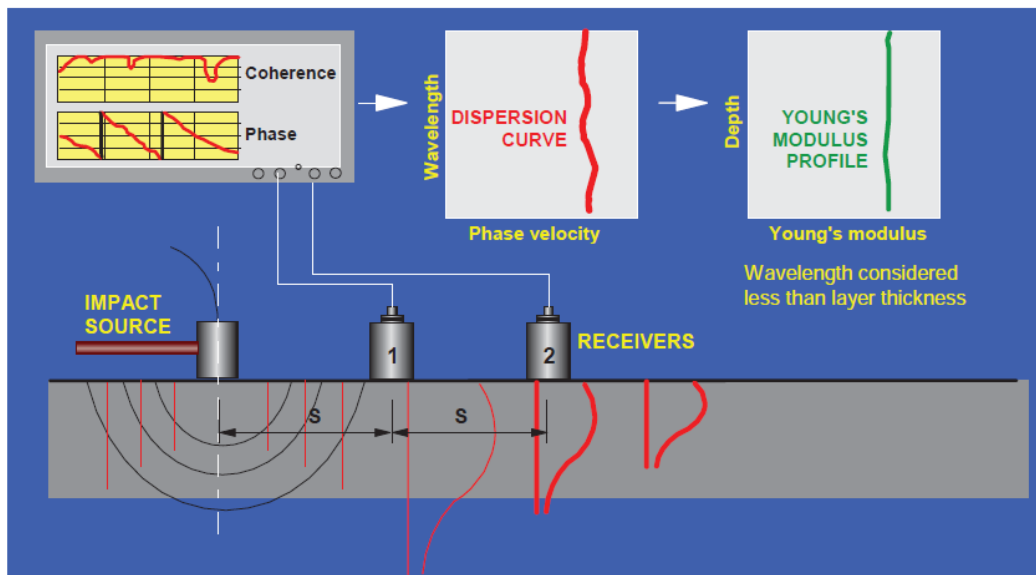


Figure 02: The Procedure of Elastic Modulus Measurement by PSPA.

According to the definition introduced by Dr. Nazarian at 1984 [2]: “Assuming vertical velocity variation, each frequency component of a surface wave has a different propagation velocity (called phase velocity, C_1) at each unique frequency (f) component. This unique characteristic result in a different wavelength (A) for each frequency propagated. This property is called dispersion.” The dispersion properties of surface wave can be used to generate dispersion curves (Wavelength vs Phase velocity), if we assumed the material properties are uniform, such as the density and Poisson's ratio, the Young's modulus profile (Depth vs Young's modulus) can be generated according to the above equation. Furthermore, the surface wave velocity propagation is independent of wavelength when the wavelengths is less than or equal to the thickness of the uppermost layer [35]. Therefore, the elastic modulus of the material in the uppermost layers is determined without an inversion or back calculation algorithm.

To collect data with the PSPA, the high-frequency source is activated four to six times. Prerecording impacts of the source are used to adjust the gains of the amplifiers in a manner that optimizes the dynamic range of the electronics. The outputs of the three transducers from the final three impacts are saved and stacked [35]. Typical voltage outputs (time records) of the three transducers are shown in Figure 03. An actual variation in elastic modulus with wavelength (dispersion curve) from the time records shown in Figure 03 is demonstrated in Figure 04. In practical reasons, the wavelength is simply relabeled as depth [35]. In that manner, the operator of the PSPA can obtain a qualitative feel for the variation in modulus with depth. As approximated by the solid line, the modulus is reasonably constant for the first 4 inches, below which the modulus tends toward lower values with depth. To obtain the average elastic modulus, the modulus from a wavelength of about 2 inches to slightly less than the normal thickness of the top layer (8 inches) is used. Furthermore, the following relationship was used to adjust the elastic modulus of asphalt or asphalt concrete overlays to a reference temperature of 77°F (25°C):

$$E_{77} = \frac{E_t}{1.35 - 0.0078(t - 32)}$$

Where E_{77} and E_t are the modulus at 77°F [37].

In practice, the quality of the ultrasonic surface wave (USW) data is affected significantly by several aspects:

- The surface condition of the bridge deck and pavement, such as cracking or rough surface.
- The improper operations of the instrument during the field testing, such as poorly coupled of the instrument to the testing surface.
- The elastic modulus measurement of asphalt or asphalt concrete overlays is affected significantly by temperatures.
- The USW test is interested in a narrow high frequency range in which the traffic does not affect the quality of test results.

In case of relatively homogeneous materials, such as concrete or asphalt, the velocity of the surface wave or phase velocity does not vary significantly with frequency. The surface wave velocity can be precisely related to the material elastic modulus using either the assumed or measured mass density and Poisson ratio of the material. An average velocity (Vertical red line shown in Figure 04) is used to correlate it to the concrete modulus of the top layer. Significant variation in the phase velocity will be an indication of the presence of a deterioration anomaly. However, the elastic modulus evaluation becomes more complicated for multiple layered systems, such as pavements or bridged decks with asphalt concrete overlays, where the elastic modulus of each layers differ significantly [18].

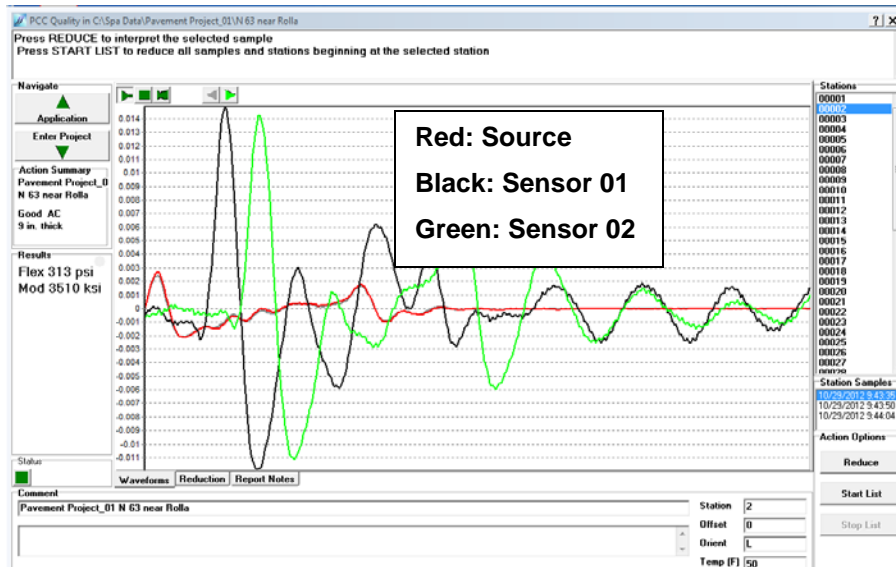


Figure 03: Typical Time Records of Three Transducers.

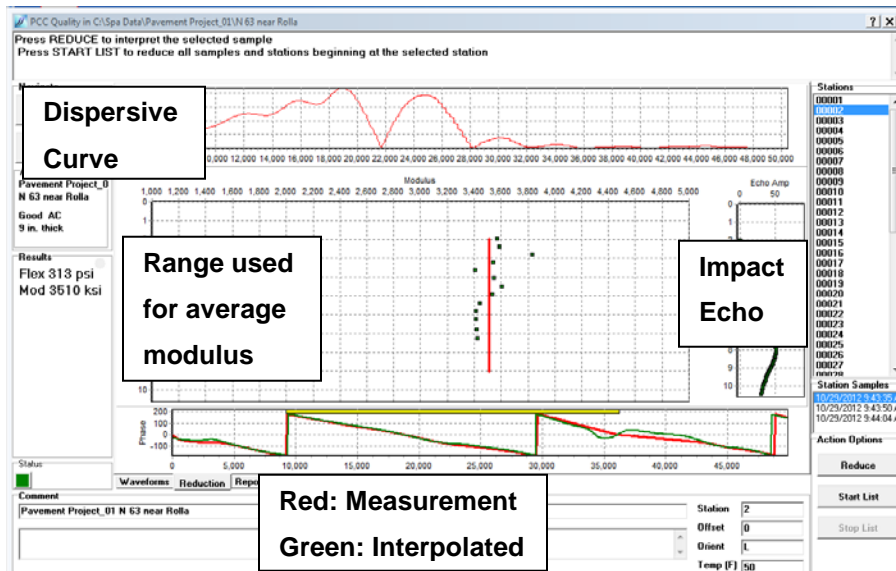


Figure 04: Typical Dispersion Curve Obtained from the Time Records in Figure 03.

1.1.2 Impact Echo

The impact echo method is a non-destructive technique (NDT) for flaw detection in concrete [5]. Thus, it is used to detect defects in the structure and can be thought of as a diagnostic tool in defect identification. The high-frequency impact source and the nearby transducer of PSPA instrument are used to conduct the impact-echo tests in the field. The configuration of impact-echo testing is shown in Figure 05. The estimation of P-wave velocity by measuring the travel time of P-wave between two transducers is often difficult since the P-wave arrivals is difficult to identify in the time records.

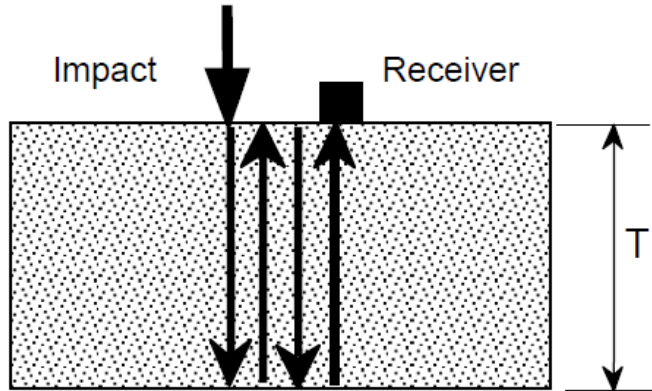


Figure 05: The Configuration of Impact Echo Testing.

A more reliable procedure to estimate P-wave velocity is through measurement of the surface wave velocity (V_R) from ultrasonic surface wave test since the relationship between P-wave velocity and surface wave velocity can be determined if the properties of the uppermost layers assumed to be uniform:

$$V_p = \sqrt{\frac{2(1-\nu)}{1-2\nu}} \times (1.13 - 0.16\nu)VR$$

Where

V_R = velocity of surface waves,

ν = Poisson's ratio

V_p = P-wave velocity

The elastic waves are generated when the mechanical impact is applied on the surface of the material. Because of a significant contrast in rigidity of concrete and air, the elastic wave is practically or entirely reflected off the bottom of the deck back to the deck surface. The frequency of the reflection, called return frequency, can be identified in the response spectrum of the recorded signal [20]. Thus, the depth of the reflector, in this case the deck thickness, can be obtained from the return frequency and the previously determined P-wave velocity, as illustrated in Figure 05. The relationship between P-wave velocities, return frequency f and deck thickness T can be determined simply by this equation:

$$f = \frac{Vp}{2 * T}$$

The Figure 06 has shown the example of amplitude spectrum (frequency spectrum) contrast between intact and deboned concrete slabs. For the case of the intact slab, a large portion of input energy is reflected back from the bottom of the slab or concrete base interface. Some of the energy is transmitted into the base and subgrade. For the case of the deboned slab, a portion of the energy will be reflected from the concrete-air interface created by the deboning.

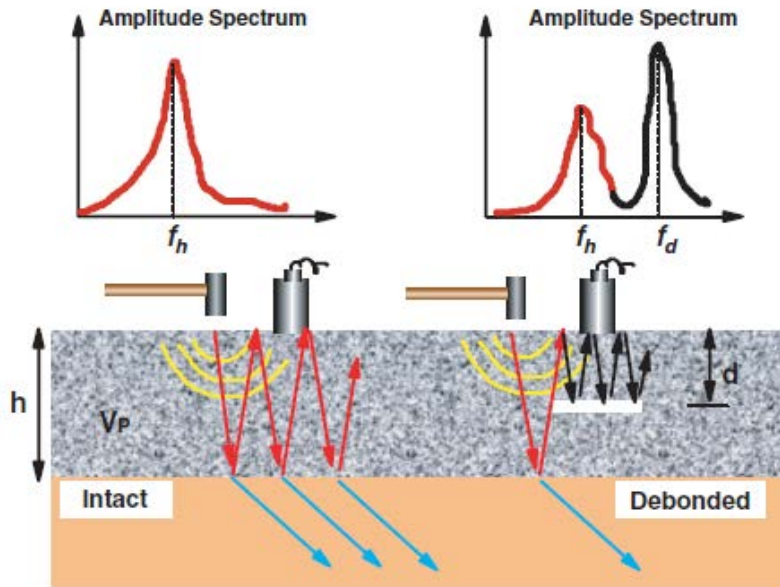


Figure 06: The Amplitude Spectrum Contrast between Intact and Debonded Concrete Slabs.

Therefore, other than the full slab thickness frequency f_h , the amplitude spectrum will show one or more frequency peaks at $f_d = \frac{V_p}{2d}$, corresponding to the frequency of reflections from the debonding at a depth of $d < h$. The relative amplitude of the peaks depends on a number of factors, including the extent, depth, continuity, and position of debonding, as well as the frequency content of the impact source [21].

In practice, the interpretation of amplitude spectra is not always straightforward. The complex internal structure of bridges and pavements, such as reinforcement steel or construction joint can generate high level ambient noise. Furthermore, the P-wave velocities used for impact-echo data analysis derived from surface wave velocities are not accurate due to several reasons: First of all, the propagation direction of P-wave and surface wave velocities in concrete or asphalt material are significant different. Second, the improper estimated of material properties, such as Poisson ratio, can also affect the accuracy of P-wave velocity calculations.

1.2. PSPA DATA ACQUISITION

The field implementation of PSPA testing in bridge decks or pavements evaluation are conducted based on point loading test system in a grid of selected spacing. The dense spacing can provide more detail analysis with time consuming for data acquisition, processing and interpretation. The field evaluation of bridge decks is typically done on grids spacing of 2×2 feet to 3×3 feet [20]. The grid spacing of 2×2 feet has been selected for PSPA data collection in this study for bridge decks evaluation. A bridge deck evaluation using 2×2 feet grid spacing has been shown in Figure 07. The time consuming for each test point generally taken less than 30 seconds.

According to a previous study conducted by Dr. Gucunski at 2008 [20], the 50 m² of the deck surface can be tested per hour with 3×3 feet grid spacing or 20 m² with 2×2 feet grid spacing. In this study, the location and scale of the PSPA test grid is varied based on the several factors: speed of data acquisition, the severity degree of the bridge and the scale of the bridge. Furthermore, the selection of PSPA testing grid is also depend on the visual and ground penetration radar inspection results.

The length of PSPA test for pavements evaluation in this project is 1000 feet. A 100 feet interval is conducted for PSPA data collection in longitude direction of the pavement. The half lane of the pavement is covered by PSPA test point with 2 feet intervals in traverse direction. The investigation width of the pavement is 10 feet. The field data acquisition procedure has been shown in Figure 08. The location and scale of PSPA test for pavement evaluations is mainly based on several factors: speed of data acquisition, the material type of top pavement layers and the severity degree of the pavement.

In order to mitigate the potential problems of PSPA data acquisition statement in previous section, the locations of reinforcement steel are marked before conducted PSPA field tests. The PSPA instrument has been placed avoid overlaid on the top of reinforcement steels during the field tests of bridge decks evaluation.



Figure 07: PSPA Data Acquisition on the Bridge Deck with 2×2 feet Grid Spacing [18].



Figure 08: PSPA Data Collection in the Field for Pavement Evaluation.

1.3. PSPA DATA PROCESSING AND INTERPRETATION

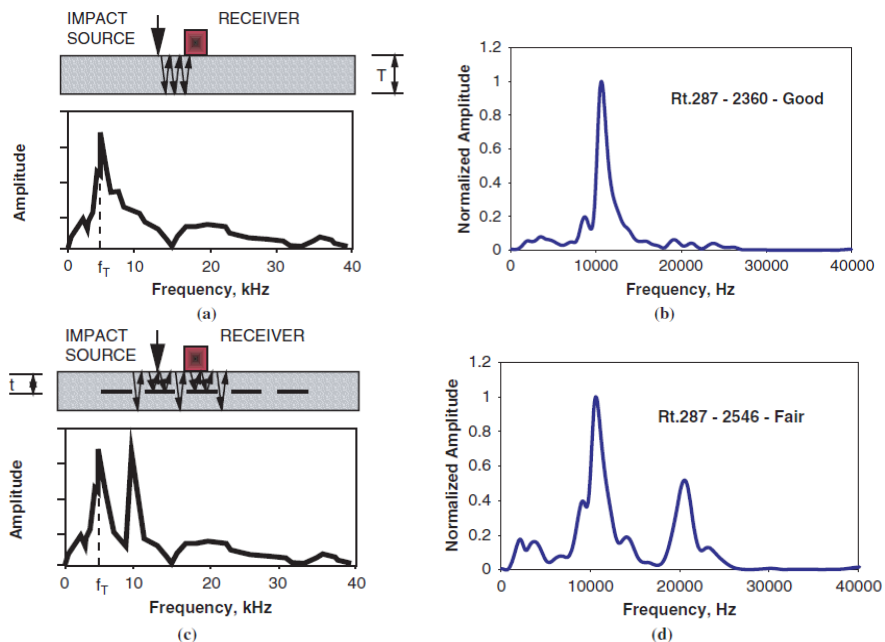
1.3.1 Ultrasonic Surface Wave

For each PSPA testing point, the dispersion curve can be generated automatically and rapidly after the field test conducted. Variation in the phase velocity would be an indication of variation of material properties (elastic modulus) with depth. Once the surface wave velocity is determined, it can be well correlated to both compression and shear wave velocities, and thus to the Young's and shear modulus [20]. When the surface waves propagating through the delamination or deterioration area of bridge decks or pavements, the surface wave velocity is reduced significant. Therefore, the deterioration of bridges and pavements can be identified from the variation of elastic modulus with depth.

However, the quality of ultrasonic surface wave (USW) data can be easily affected by the surface condition, weather and improper operations. Furthermore, the USW method cannot provide reliable elastic modulus values on deteriorated areas of concrete decks or pavements, such as delaminated or debonded sections. For the multiple layers system, such as asphalt concrete overlays, the interpretation of USW modulus becomes significantly more complicated. Therefore, the extensive experiences are required for understanding and interpreting test results. Furthermore, the construction of 2D contour map of elastic modulus for each test sections also needs experience and extensive time consuming. The deterioration sections of decks or pavements can be identified and characterized relatively low elastic modulus.

1.3.2 Impact Echo

In the case of a delaminated deck, reflections of the P-wave occur at shallower depths causing a shift in the response toward higher frequencies. Depending on the extent and continuity of the delamination, the partition of energy of elastic waves may vary and different grades can be assigned to that particular section of a deck as a part of the condition assessment process [20]. The grades selection based on the various degree of deck delamination has been shown in Figure 09. In the case of a sound deck (one in good condition, Figure 09a and 09b), a distinctive peak in the response spectrum corresponding to the full depth of the deck can be observed, as shown by two spectra under the cross section of the bridge deck. Figure 09a represents a schematic of the expected spectrum, while Figure 09b is taken from actual field testing. Initial delamination (deck in fair condition, Figure 09c and 09d) is described as occasional separation between the two deck zones. It can be identified through the presence of two distinct peaks, indicating energy partition from two dominant wave propagation patterns. The first peak corresponds to reflections from the bottom of the deck, while the second corresponds to reflections from the delamination. Progressed delamination (deck in poor condition, Figures 09e and 09f) is characterized by a single peak at a frequency corresponding to a reflector depth that is shallower than the deck thickness, indicating that little or no energy is being propagated toward the bottom of the deck. Finally, in a very severe case of a wide delamination (serious condition, Figures 09g and 09h), the dominant response of the deck to an impact is characterized by a low-frequency response of flexural-mode oscillations of the upper delaminated portion of the deck. This response is almost always in the audible frequency range, unlike response of the deck in the fair and poor conditions, which may be in the ultrasonic range. Because this response is significantly lower than the return frequency for the deck bottom, it produces an apparent reflector depth that is larger than the deck thickness.



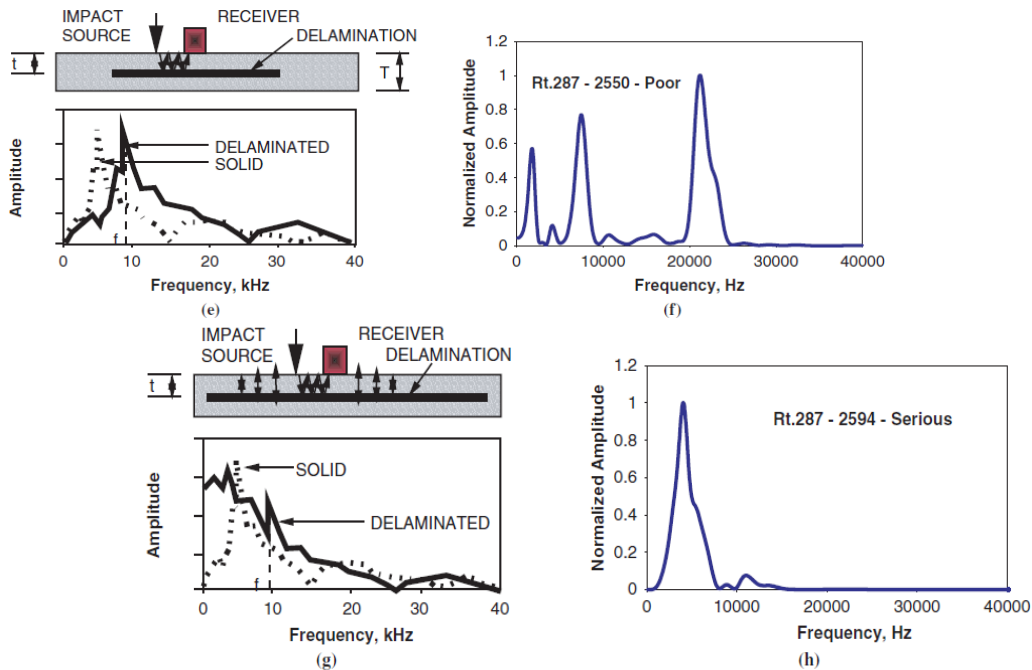


FIGURE 09: Grades for various degrees of deck delamination shown, respectively, with schematic of expected spectrum and spectrum from field testing: (a) and (b) for good (intact) condition, (c) and (d) for fair condition, (e) and (f) for poor condition, (g) and (h) for serious condition [20].

In practice, the processing and interpretation of the IE data is not always straightforward. In the case of a slab in marginal condition, the spectrum exhibits several frequency peaks, which may introduce ambiguity in the interpretation of the test results (e.g., Figure 09e and 09f). Furthermore, the complex structure (reinforcement steel or construction joint) of the bridge deck or pavement with the heterogeneous nature of reinforced concrete or asphalt introduced a high level of ambient noise, which can significantly effects the interpretation of the IE spectrum. Finally, the automatic thickness calculation results provided by the PSPA software have been demonstrated not accurate compared with Lidar and borehole test results. There are several factors can affect the accuracy of the thickness calculation: First of all, the P-wave velocity used for thickness calculation derived from surface wave velocity has been demonstrated is not accurate. Second, the difficult of IE spectra interpretation can also affect the accuracy of thickness calculation. Therefore, the extensive experiences needed for impact-echo (IE) data processing and interpretation. In order to solve or mitigate current problems found in impact-echo data processing and interpretation, the following steps have been conducted in this study:

- The locations of reinforcement steel are marked before conducted PSPA field tests. The PSPA instrument has been placed avoid overlaid on the top of reinforcement steels during the field tests of bridge decks evaluation.
- The assumed uniform P-wave velocity has been used for thickness calculation instead of the automatic calculation results. The manual impact-echo data analysis results have been verified more efficient and accurate than automatic analysis results by comparing with the Lidar test results.

- The first frequency peak in the IE spectrum has been identified as the bottom reflection from the deck or pavement layers bottom used for the thickness calculation instead of return frequency (the strongest reflection) in order to avoid the effect of high level ambient noise. The manual impact-echo data analysis results have been verified more efficient and accurate than automatic analysis results by comparing with the Lidar test results.

Furthermore, the construction of 2D reflection depth map from the bottom of the decks for each test sections also needs experience and extensive time consuming. The deterioration area of decks can be identified and characterized with apparent reflection depth that is large than the deck thickness.

2. SCOPE OF THE WORK

- Implementing PSPA field tests on different materials (concrete, asphalt overlaid concrete, asphalt) type of bridge decks and pavements.
- Conducting PSPA data processing and interpretation for all bridge decks and pavements. For each bridge decks or pavement sections, comparing the PSPA data results with other NDT data results (GPR and Lidar) and coring controls.
- Evaluation the accuracy of PSPA data for defects detection for each bridge decks and pavements. Identifying and characterizing the current problems or limitations found during the PSPA data processing and interpretation procedures, such as the effect of reinforcement steel to the PSPA data results or the effect of current P-wave velocity determination method to the accuracy of IE data results.
- Conducting the valid test in the laboratory with the simulation concrete slabs (known the location of reinforcement steel and delamination). Confirm the effect of reinforcement steels to the PSPA data results, adjustment or modification the current procedures of PSPA data processing and interpretation in order to improve the accuracy of PSPA data results, such as building the uniform scale for elastic modulus data based on the statistical analysis or employment the uniform estimation P-wave velocities instead of the variation P-wave velocities transformed from the surface wave velocities.
- Comparing the modification PSPA data results with the ground truth data. Evaluation the performance of PSPA methods for the rapid condition assessment of bridge decks and pavements based on the several factors: speed of data acquisition, accuracy and easy to use.
- Creating the general protocol for the proper and effective use of PSPA methods for the rapid condition assessment of bridge decks and pavements in the future.
- Comparing the PSPA data results with ground penetrating radar (GPR) data results for some of bridge decks and pavement sections.

3. TIMELINE TABLE

In this study, twelve bridges and eight pavement sections located at multiple locations of Missouri State have been selected to conduct PSPA field tests. Table 01 summarized the PSPA data acquisition date and location for all the bridges and pavement sections with the name of operator in the field.

Bridge decks investigation						
Done	Name of Project	Location of Project	Start Date	End Date	Operator	
X	A1187	Jefferson City, MO	9/16/2012	9/16/2012	Mengxing Li	
X	A1297	Sedalia, MO	10/24/2012	10/24/2012	Mengxing Li	
X	A1193	Syracuse, MO	11/7/2012	11/7/2012	Mengxing Li	
X	A1479	Lake Ozark, MO	11/8/2012	11/8/2012	Mengxing Li	
X	A2966	Mountain Grove, MO	10/16/2012	10/16/2012	Mengxing Li	
X	A3405	Saint James, MO	11/14/2012	11/14/2012	Mengxing Li	
X	A3406	Saint James, MO	11/15/2012	11/15/2012	Mengxing Li	
X	K0197	Saint James, MO	11/28/2012	11/28/2012	Mengxing Li	
X	K0656	Jefferson City, MO	11/26/2012	11/26/2012	Mengxing Li	
X	A1187	Jefferson City, MO	5/19/2013	5/19/2013	Nwokebuihe Stanley C.	
X	A2111	Fulton, MO	5/23/2013	5/23/2013	Mengxing Li	
X	A3017	Warsaw, MO	6/6/2013	6/6/2013	Nwokebuihe Stanley C.	
Pavements Section investigations						
X	Section 01	US 63 Rolla MO	10/29/2012	10/29/2012	Mengxing Li	
X	Section 02	US 54 Camden City	11/12/2012	11/12/2012	Mengxing Li	
X	Section 03	MO 179 Jefferson City	12/3/2012	12/3/2012	Mengxing Li	
X	Section 04	Hwy Franklin MO	7/25/2013	7/25/2013	Mengxing Li	
X	Section 05	I-55 Pemiscot County	7/31/2013	7/31/2013	Mengxing Li	
X	Section 07	Hwy U Dent County	3/13/2013	3/13/2013	Mengxing Li	
X	Section 08	I-35 N Cameron MO	8/7/2013	8/7/2013	Mengxing Li	
X	Section 06	I-55 St. Louis City	9/23/2013	9/23/2013	Mengxing Li	

4. EXPECTANCE OUTCOME

Twelve bridge decks and eight pavement sections have been selected to implement PSPA field tests in this study. The example of PSPA test data results on bridge decks and pavement sections have been presented in the following sections.

4.1 PSPA DATA RESULTS OF THE BRIDGE A1479

The concrete bridge A1479 is located on the state highway US 54 W over Osage River. The bridge was constructed in 1966 with the total lengths of 869.1 ft with the deck width of 34.5 ft. The bridge deck is composed of six concrete spans with two lanes. The appearance of the bridge has been shown in Figure 10.



Figure 10: The Appearance of the Concrete Bridge A1479.

Six PSPA test grid areas (10 × 4 ft) with 2 × 2 ft grid spacing have been selected to conduct PSPA field tests on the bridge deck of A1479 has been shown in Figure 11. One of the PSPA test results, section D compared with Lidar and GPR test results will be presented in the following sections.

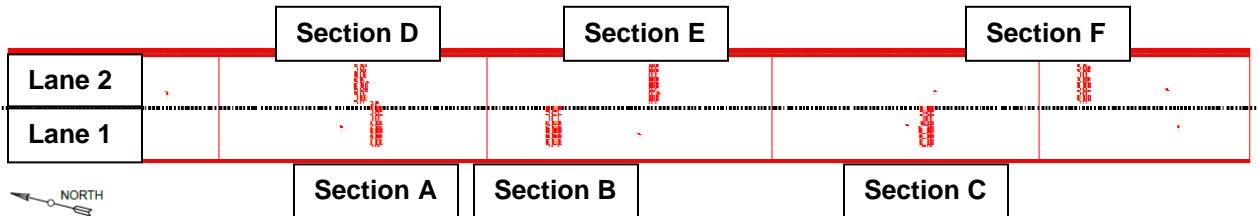


Figure 11: The Selected PSPA Tests Area for the Bridge A1479.

The contrast typical time records of PSPA data between delaminated concrete (a) and intact concrete (b) has been shown in Figure 12.

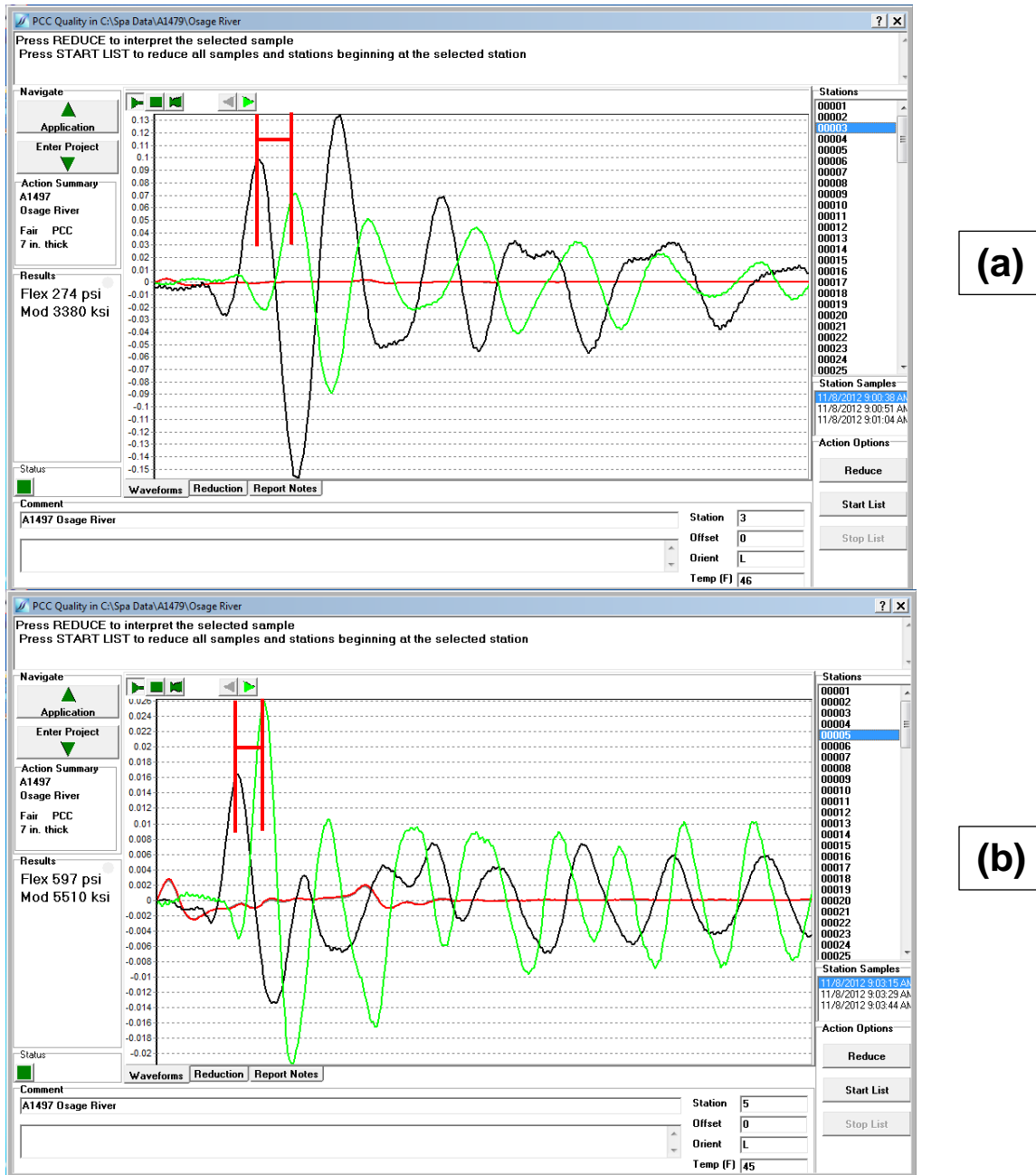


Figure 12: The Time Records (waveform) of Delaminated Concrete (a) and Intact Concrete (b)

For the delaminated concrete, the time difference (the distance between two vertical red lines) between two surface wave peaks is obviously wider than the intact concrete. Thus, the propagation of surface wave velocity in delaminated concrete will be much slower comparing with the intact concrete. And the elastic modulus of delaminated concrete will be much lower than intact concrete.

The typical dispersive curves contrast between intact concrete (c) and delaminated concrete has been shown in Figure 13. The average elastic modulus (the vertical red line) of delaminated concrete is significant lower compared with the intact concrete.

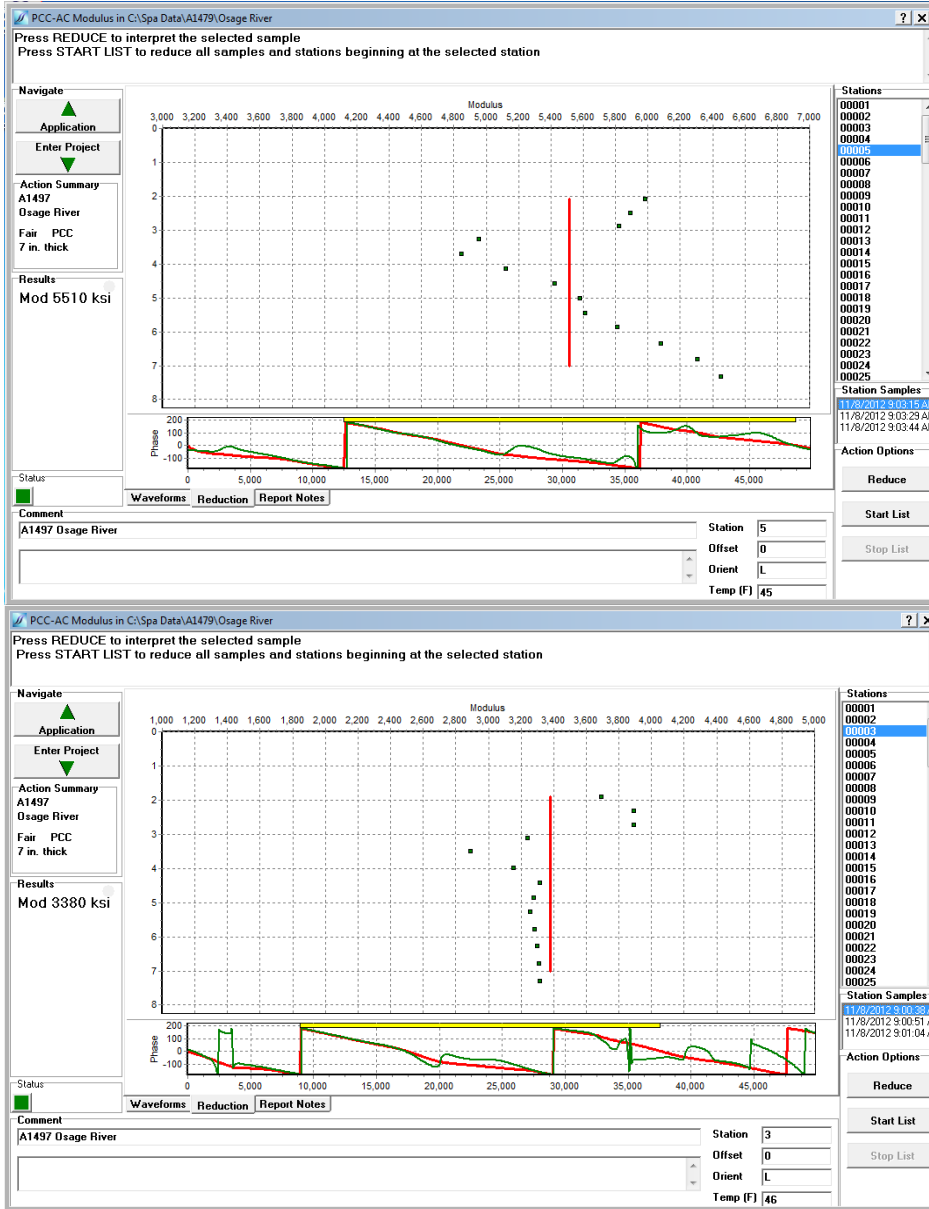


Figure 13: The Dispersion Curves of Intact Concrete (c) and Delaminated Concrete (d).

Figure 14 shown the typical frequency spectrum contrast between intact concrete (e) and delaminated concrete (f). The influence of reinforcement steel to impact echo data interpretation is significant. Furthermore, the frequency spectrum difference between delaminated and intact concrete can be observed from several aspects: First of all, the bottom reflection frequency of delaminated concrete is much lower than intact concrete. Second, the frequency distribution range for delaminated concrete (5-33 kHz) is also much lower than intact concrete (10-50 kHz). Last, the shape of frequency distribution for delaminated concrete is wider than intact concrete.

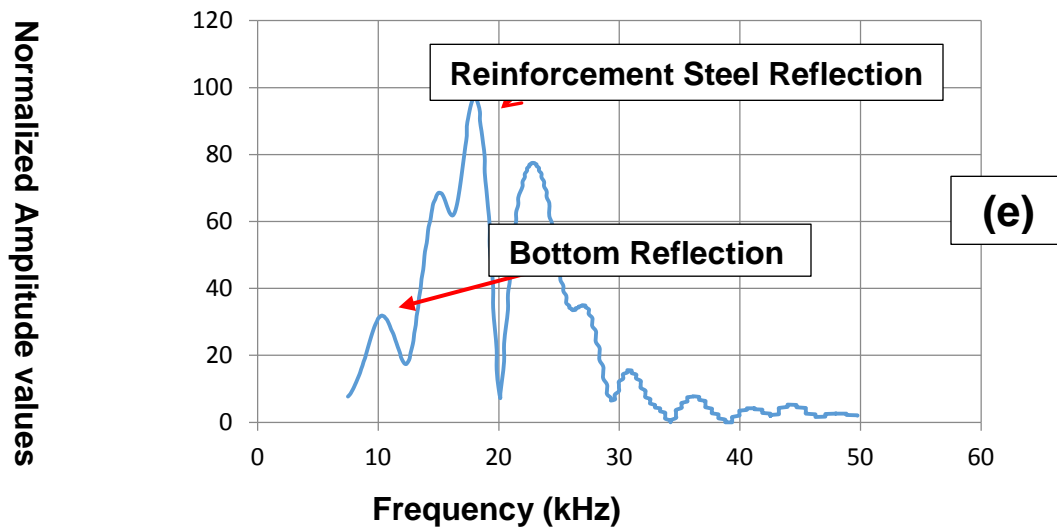
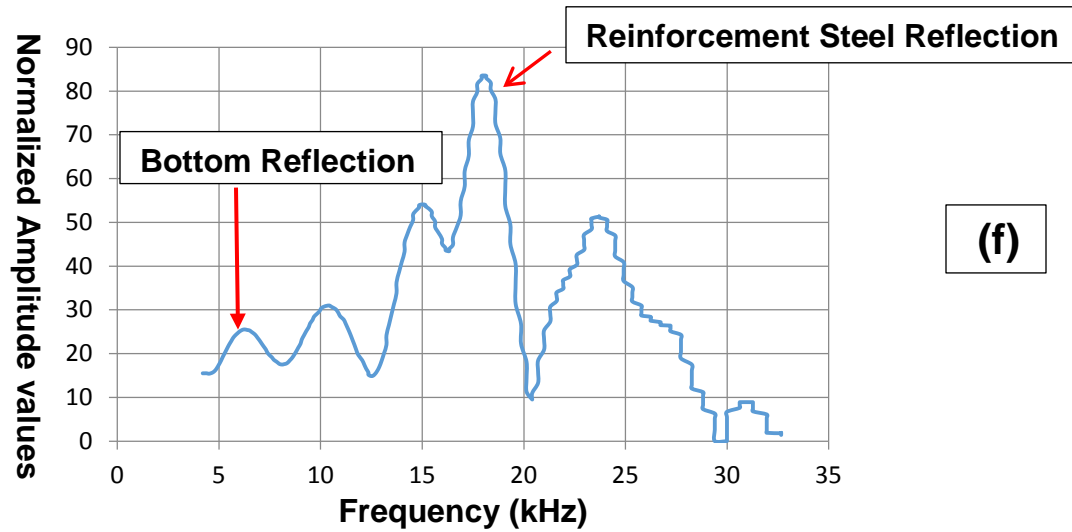


Figure 14: The Frequency Spectrum of Intact Concrete (e) and Delaminated Concrete (f).

The hydro-demolition test (Figure 15) and ground penetrate radar scan has been carried out for the entire bridge in order to verify the PSPA test results. Furthermore, the Lidar scan has been conducted with hydro-demolition test for the entire bridge in order to map the depth difference between the intact concrete and delaminated concrete.



Figure 15: The Bridge Deck Surface after Conducted Hydro-demolition Test.

4.1.1. Ultrasonic Surface Wave Data Interpretation.

2D contour map of average elastic modulus distribution for each PSPA test sections has been generated in order to obtain a better understanding of deterioration conditions for the entire bridge deck. One of the modulus contour map (section D) compared with Lidar and GPR test results has been demonstrated in Figure 16. For Lidar data map, the deterioration condition of the bridge deck represented by the different colors (a). The blue color represented the good condition and the orange with green color represented the severe and poor condition. Furthermore, the red spots in the map represented each PSPA point test locations in the field. For PSPA data map, the deterioration condition of the bridge deck represented by different modulus range. Low elastic modulus range with purple color represented the severe condition, and the high elastic modulus range with blue color represented the good condition. For GPR map, the green color area represented the moderate deterioration condition, and the yellow or orange area represented the poor condition. The deterioration area shown in the elastic modulus map correlated very well with the Lidar results. Thus, the accuracy of USW method for bridge deck assessment has been demonstrated.

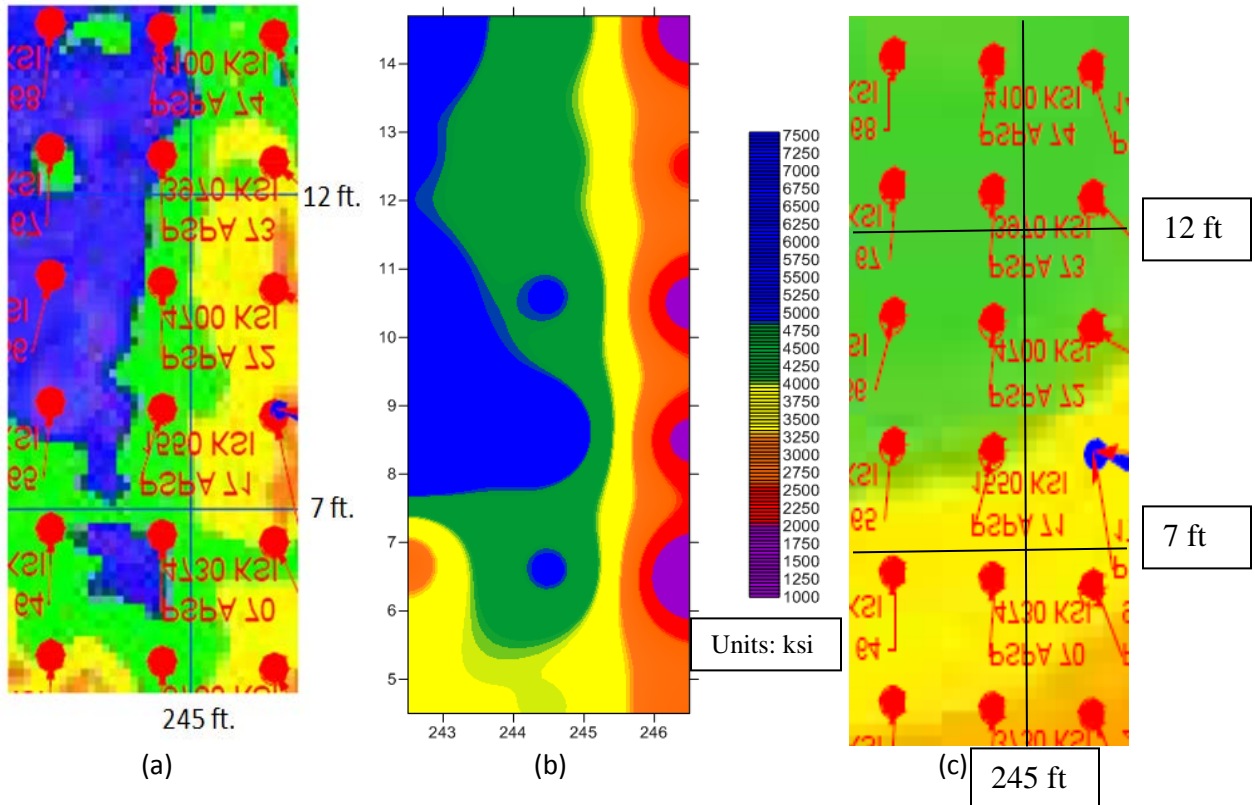


Figure 16: The Comparison Data Results of Test Section D among Lidar Data (a), PSPA Data (b) and GPR Data (c).

4.1.2. Impact Echo Data Interpretation.

The first frequency peak on the frequency spectrum has been identified as the reflection frequency from the bottom of the bridge deck. For delaminated concrete, the deck thickness will much thicker than intact concrete and out of normal range of the deck thickness based on the previous calculation equations. 2D bridge deck thickness reflection map compared with Lidar test results has been shown in Figure 17. Based on the principles of PSPA, the P-wave velocity estimated from the surface wave velocity, thus, the P-wave velocity in the delaminated concrete will much slower than intact concrete. The test results of 2D deck thickness map (f) based on the PSPA principle has been demonstrated is not accurate compared with Lidar test results. Several reasons can be explained for the inaccurate test results. First of all, the propagation direction of P-wave (vertical) and Surface wave (horizontal) in the concrete slab is different. Second, the indirect calculation procedures based on previous equations will cause the overestimate P-wave velocity results. Thus, the uniform P-wave velocity (3800m/s) instead of current P-wave velocity has been used for the calculation of deck thickness based on the bottom reflection frequency values obtained from impact-echo data. The new 2D reflection map (e) has been demonstrated more accurate and effective than automatic PSPA test results compared with the Lidar test results.

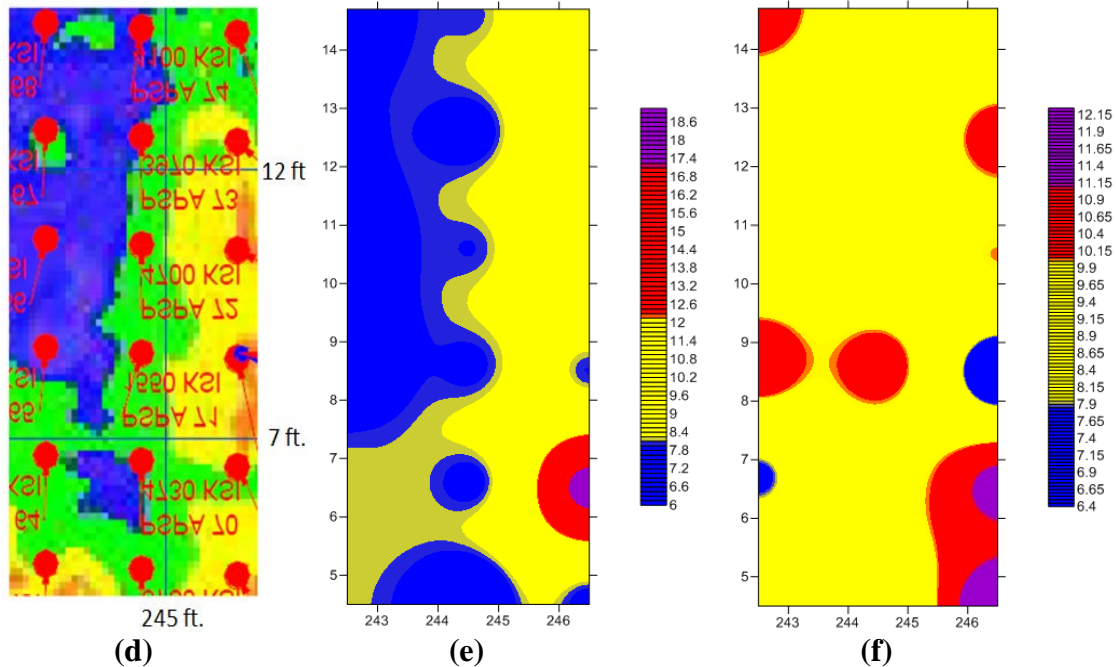


Figure 17: The Comparison Test Results between Lidar Data (d), Impact Echo Data (Manual) and Impact Echo Data (Automatic).

4.2. PSPA DATA RESULTS OF PAVEMENT SECTION 05

The pavement section 05 is located on the interstate highway 55 south bound at Pemiscot County MO. Interstate 55 was originally constructed in the 1970s, and the investigation section is composed of fully concrete. Figure 18 has shown the PSPA testing procedure on pavement section 05. The PSPA test grid generated on pavement section 05 with 100 ft intervals in wheel path direction and 2 ft intervals in traverse direction. Figure 19 shown the sketch of PSPA data collection in the field. The total length of 1000 ft with half of lanes has been covered in this investigation.



Figure 18: The PSPA In-situ Testing on Pavement Section 05.

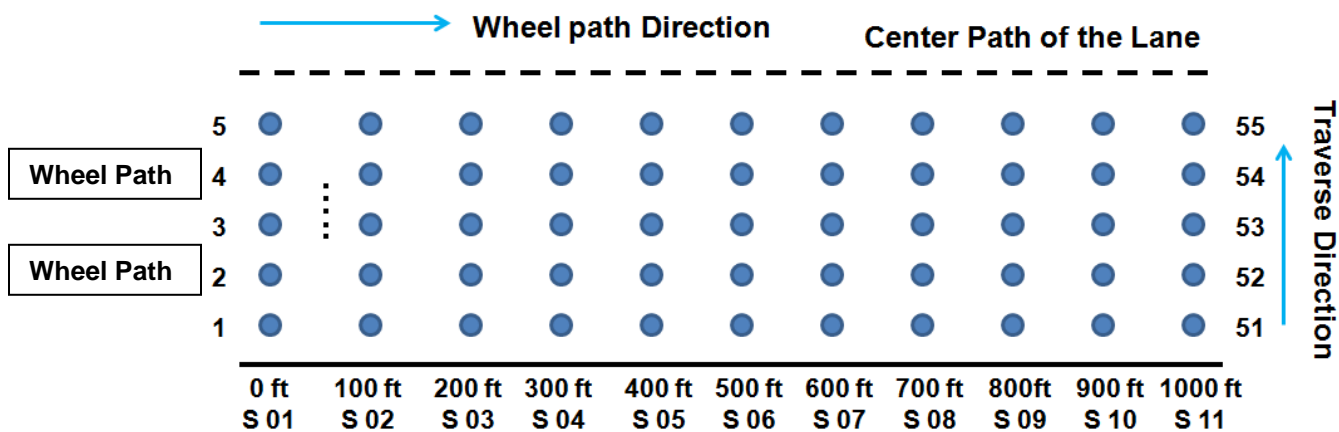
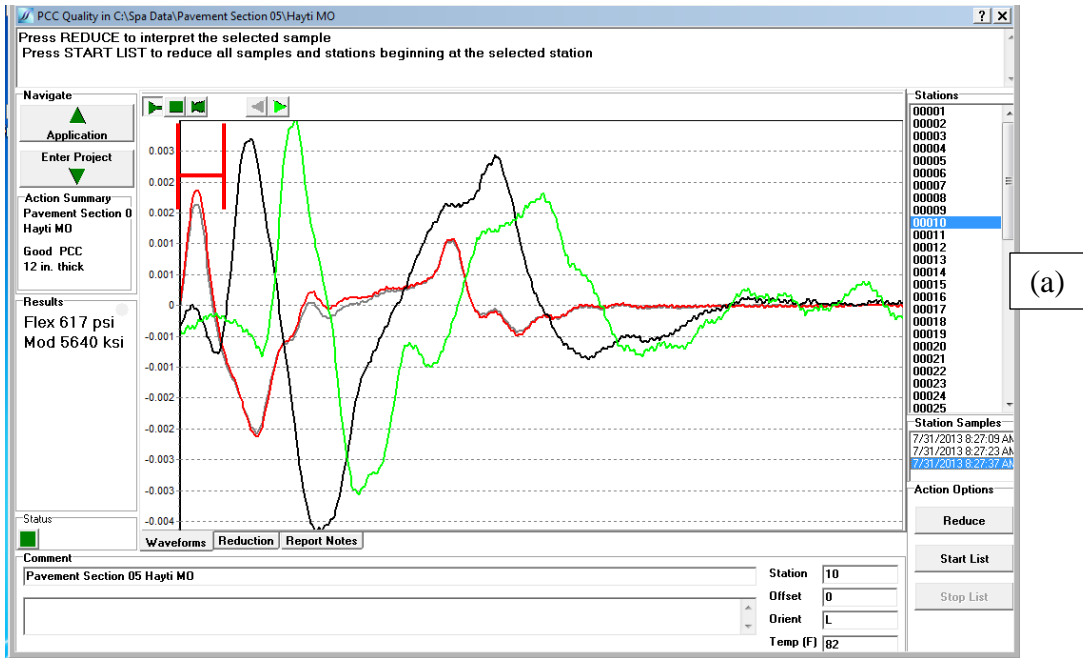
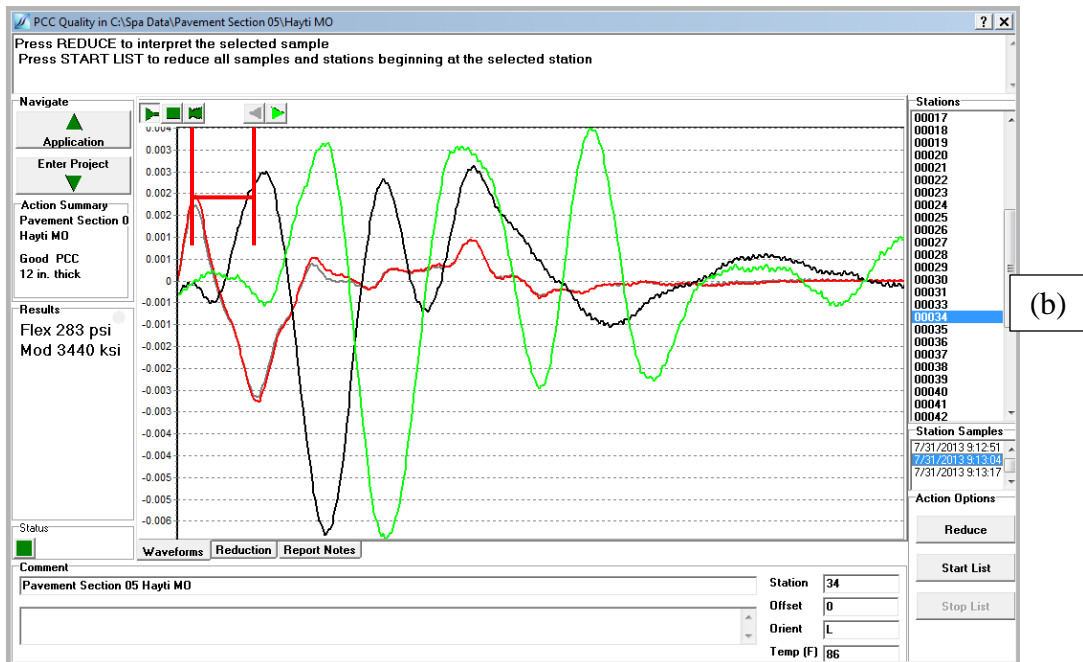


Figure 19: The Sketch of PSPA Data Acquisition in the Field (S 01 = Section 01).

The typical time records (waveform) for intact concrete layers (a) and debonded concrete layers (b) has been shown in Figure 20. The time difference (Distance between two red vertical lines) of debonded concrete is obviously wider than intact concrete. In addition, the irregularity time records of the impact source (red line) generated due to the groove structure of testing concrete surface.



(a)



(b)

Figure 20: The Typical Time Records of Intact (a) and Debonded (b) Concrete Layers.

Typical dispersion curves for intact concrete layers (c) and debonded concrete layers (d) has been shown in Figure 21. The average elastic modulus of deboned concrete is much lower than intact concrete.

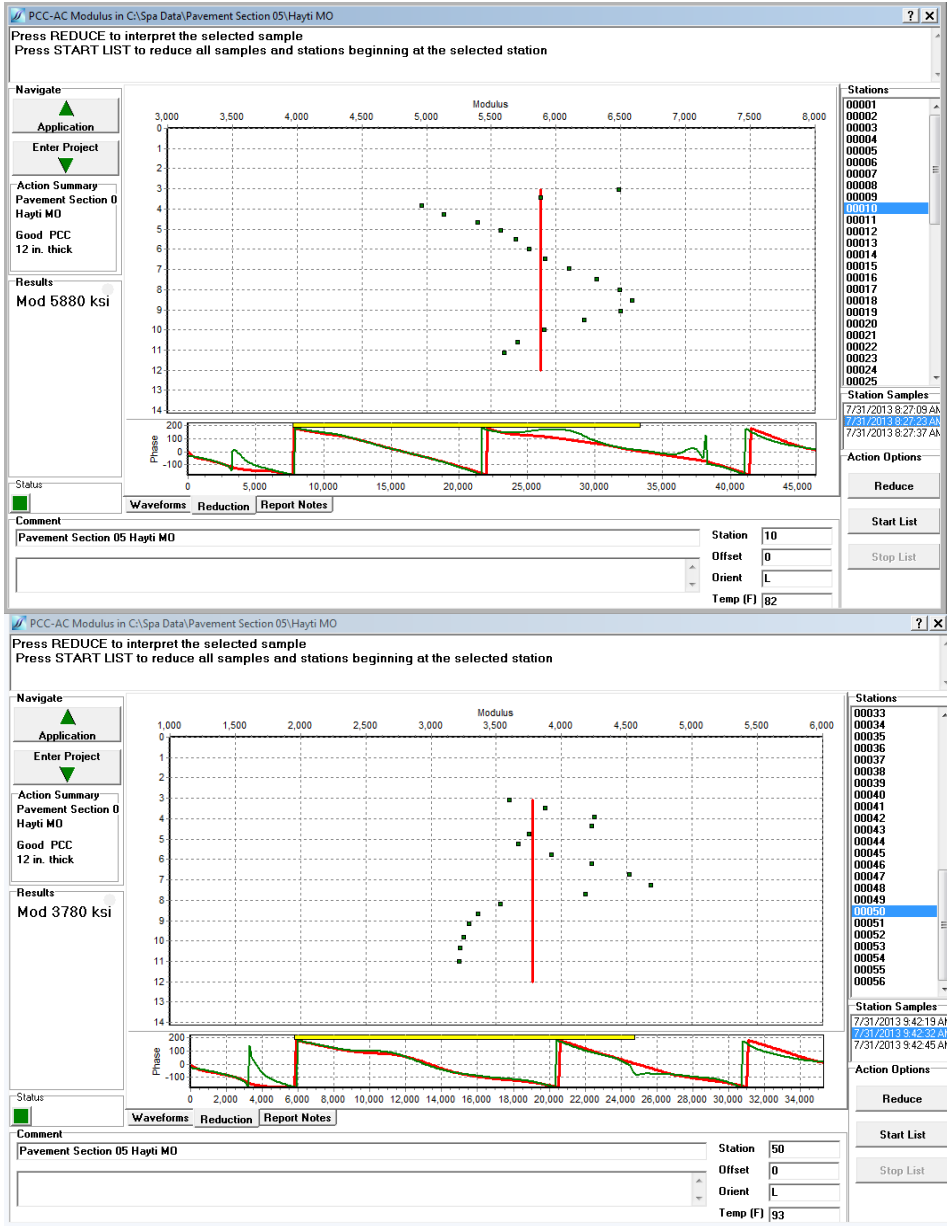


Figure 21: The Typical Dispersive Curves of Intact (c) and Debonded (d) Concrete Layers.

Typical frequency spectrums of intact (e) and debonded (f) concrete layers have been shown in Figure 22. The complex reflection singles obtained from concrete pavement section 05. However, the frequency range (3-40 kHz) of deboned concrete is relatively lower than intact concrete (5-50 kHz).

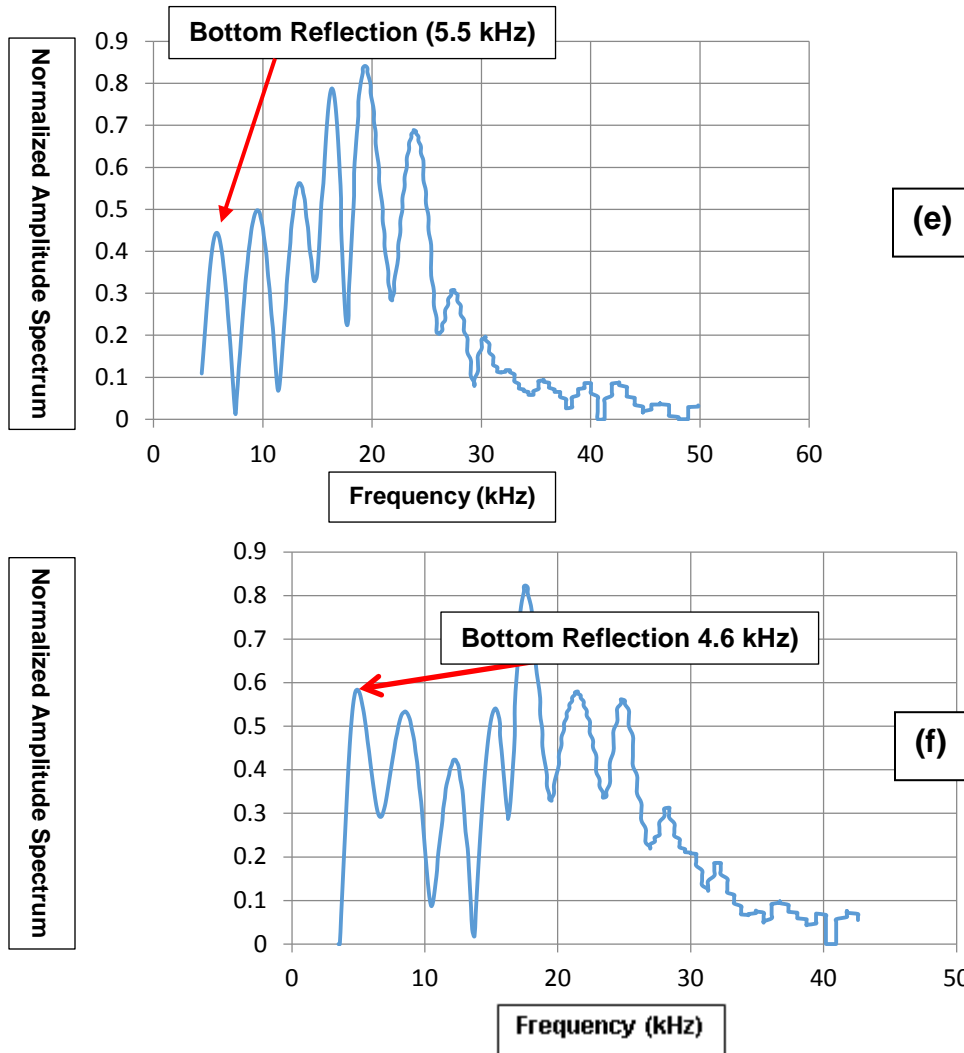


Figure 22: Typical Frequency Spectrum of Intact (e) and Debonded (f) Concrete Layers.

4.2.1. 2D Elastic Modulus Contour Map.

The 2D elastic modulus contour map for each sections has been generated in order to obtain a better understanding of elastic modulus variation with the depths. The test results of section 02 & 08 has been shown in Figure 23. Two test coring have been retrieved from section 02 & 08, both of them deboned from bottom of the first concrete layers, which are matched very well with the PSPA test results.

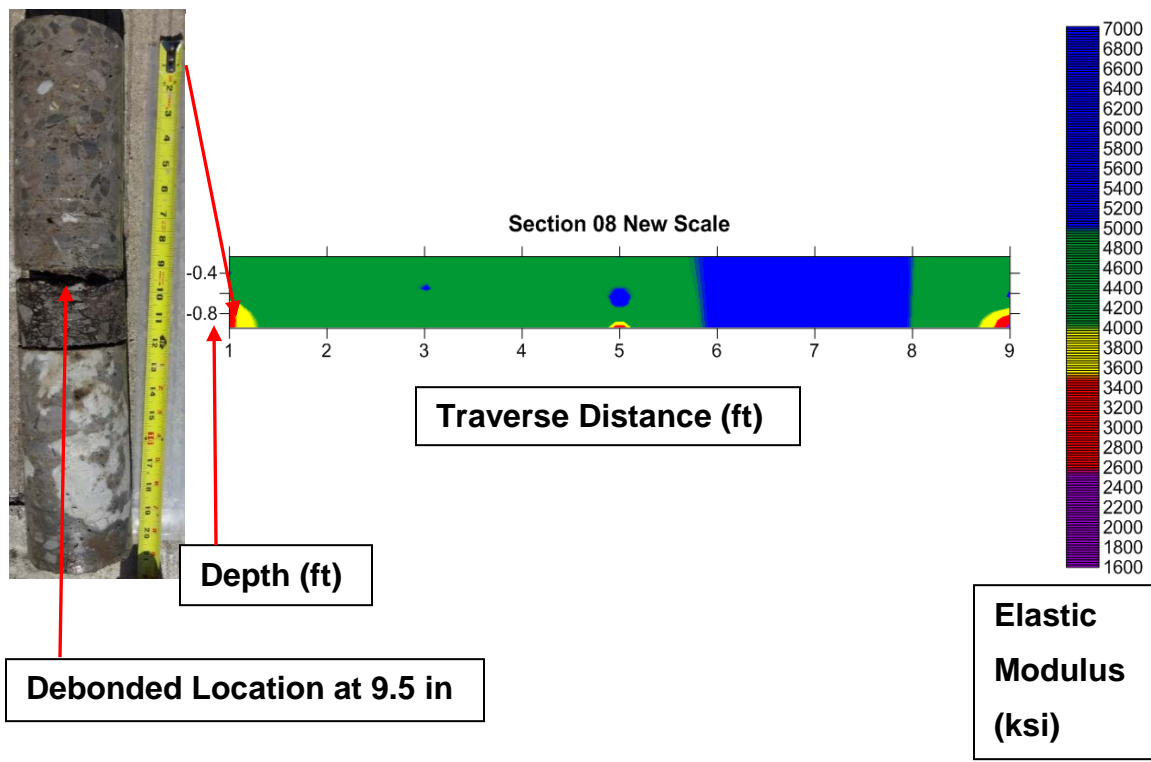
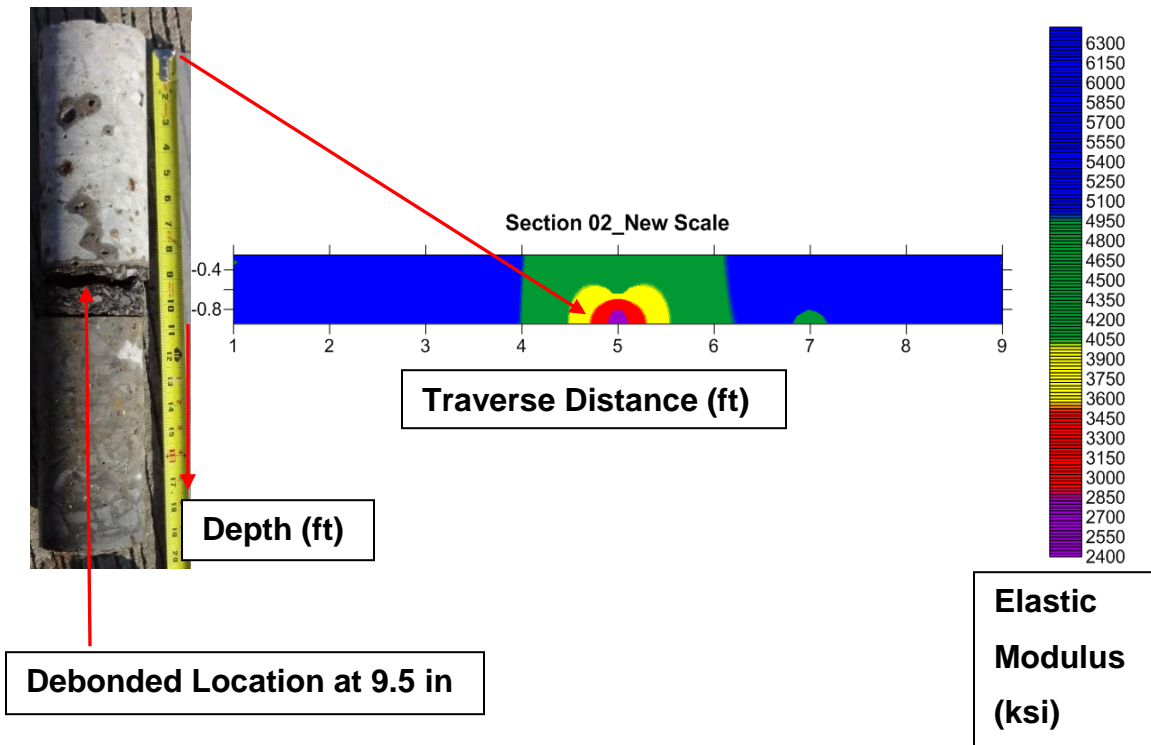


Figure 23: The 2D Elastic Modulus Contour Map Verified by the Coring Control.

4.2.2. Statistical Analysis of PSPA Data.

A statistical analysis of PSPA data for pavement section 05 has been established in order to evaluate the condition of entire pavement sections. The results shown in Figure 24 demonstrated that the lowest average elastic modulus obtained in the middle of the lane.

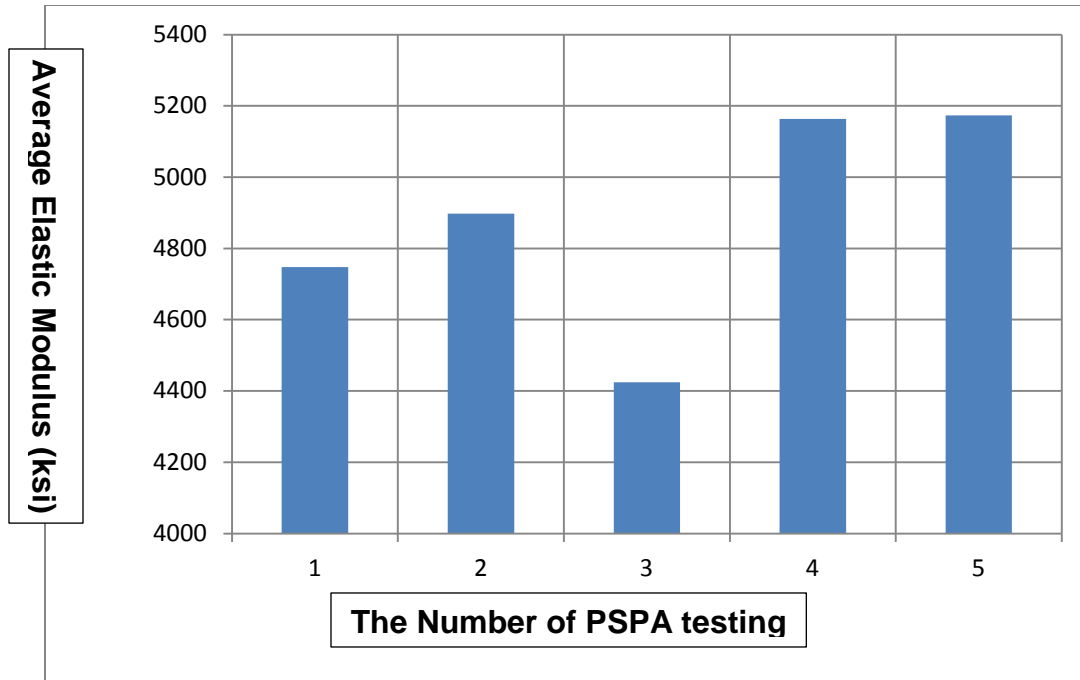


Figure 24: Statistical Analysis Results of PSPA Data.

5. REFERENCES

- [1] Sheriff, R. E., Geldart, L. P., (1995). *Exploration Seismology*, Second Edition, Cambridge University Press, NY.
- [2] Nazarian, S. *In Situ Determination of Soil Deposits and Pavement Systems by Spectral Analysis of Surface Waves Method*. PhD thesis. University of Texas at Austin, 1984.
- [3] Carino, N.J., Woodward, K.A., Leyendecker, E.V., and Fattal, S.G., 1983, "A Review of the Skyline Plaza Collapse," *Concrete International*, Vol. 5, No. 7, July, pp 35-42.
- [4] Carino, N.J., and Sansalone, M., 1984, "Pulse-Echo Method for Flaw Detection in Concrete," Technical Note 1199, National Bureau of Standards, July.
- [5] Carino, N.J., Sansalone, M., and Hsu, N.N., 1986a, "A Point Source - Point Receiver Technique for Flaw Detection in Concrete," *Journal of the American Concrete Institute*, Vol. 83, No. 2, April, pp. 199-208.
- [6] Carino, N.J., 2001, "The Impact-Echo Method: An Overview", Proceedings of the 2001 Structures Congress & Exposition, May 21-23, 2001, Washington, D.C., American Society of Civil Engineers, Reston, Virginia, Peter C. Chang, Editor, 2001. 18p.
- [7] Pratt, D. and Sansalone, M., 1992, "Impact-Echo Signal Interpretation Using Artificial Intelligence," *ACI Materials Journal*, Vol. 89, No. 2, March-April, pp. 178-187.
- [8] Carino, N.J., and Sansalone, M., 1992, "Detecting Voids in Metal Tendon Ducts Using the Impact-Echo Method," *ACI Materials Journal*, Vol. 89, No. 3, May-June, pp. 296-303.
- [9] Cheng, C. and Sansalone, M., 1993a, "The Impact-Echo Response of Concrete Plates Containing Delaminations: Numerical, Experimental, and Field Studies," *Materials and Structures*, Vol.26, No. 159, June, pp. 274-285.
- [10] Sansalone, M. and Carino, N.J., 1989, "Detecting Delaminations in Concrete Slabs with and without Overlays Using the Impact-Echo Method," *Journal of the American Concrete Institute*, Vol. 86, No. 2, March, pp. 175-184.
- [11] Lin, Y. and Sansalone, M., 1992a, "Detecting Flaws in Concrete Beams and Columns Using the Impact-Echo Method," *ACI Materials Journal*, Vol. 89, No. 4, July-August 1992, pp. 394-405.
- [12] Lin, J.M. and Sansalone, M.J., 1996, "Impact-Echo Studies of Interfacial Bond Quality in Concrete: Part I—Effects of Un-bonded Fraction of Area," *ACI Materials Journal*, Vol. 93, No. 3, May-June, pp. 223- 232.

- [13] Sansalone, M., and Streett, W. B., 1997, **Impact-Echo: Nondestructive Testing of Concrete and Masonry**, Bullbrier Press, Jersey Shore, PA.
- [14] Sansalone, M., Lin, J.M., and Streett, W.B., 1997a, "A Procedure for Determining P-Wave Speed in Concrete for Use in Impact-Echo Testing Using a P-Wave Speed Measurement Technique," *ACI Materials Journal*, Vol. 94, No. 6, November-December 1997, pp. 531-539.
- [15] Sansalone, M., Lin, J. M., and Streett, W. B., 1997b, "A Procedure for Determining Concrete Pavement Thickness Using P-Wave Speed Measurements and the Impact-Echo Method" *Innovations in Nondestructive Testing*, SP-168, S. Pessiki and L. Olson, Eds., American Concrete Institute, Farmington Hills, MI, 1997, pp.167-184.
- [16] Mori, K., Spagnoli, Y., 2002, "A new non-contacting non-destructive testing method for defect detection in concrete" *NDT&E International* , No. 35, pp 399-406.
- [17] Yeh, P., Liu, P., 2008, "Application of the wavelet transform and the enhanced Fourier spectrum in the impact echo test" *NDT&E International*, No. 41, pp 382-394.
- [18] Gucunski, N., Nazarian, S., Yuan, D., 2012, **Nondestructive Testing to Identify Concrete Bridge Deck Deterioration**, Strategic Highway Research Program (SHRP 2) report, Transportation Research Board, Washington D.C.
- [19] Yehia, S., Abudayyeh, O., 2007, "Detection of Common Defects in Concrete Bridge Decks Using Nondestructive Evaluation Techniques" *Journal of Bridge Engineering*, Vol. 12, No. 2, pp 215-225.
- [20] Gucunski, N., Slabaugh, G., 2008, "Impact Echo Data from Bridge Deck Testing" *Transportation Research Record*, No. 2050, pp 111-121.
- [21] Celaya, M., Nazarian, S., 2007, "Assessment of Debonding in Concrete Slabs Using Seismic Methods" *Transportation Research Record*, 2016, pp 65-75.
- [22] Krautkrämer, J. and Krautkrämer, H., 1990, **Ultrasonic Testing of Materials**, 4th Ed., Springer-Verlag, New York.
- [23] Sansalone, M. and Carino, N.J., 1991, "Stress Wave Propagation Methods," in *Handbook on Nondestructive Testing of Concrete*, Ed. V.M. Malhotra and N.J. Carino, CRC Press, BocaRaton, FL, pp. 275-304.
- [24] Smith, J. L., and Y. P. Virmani. 1996. Performance of Epoxy Coated Rebars in Bridge Deck. Report FHWA-RD-96-092. FHWA, U.S. Department of Transportation.
- [25] West, R.C., Zhang, J., Moore, J., 2005, **Evaluation of Bond Strength between Pavement Layers**, National Center for Asphalt Technology (NCAT) report, Auburn University, Auburn AL.

[26] Heitzman, M., Maser, K., Tran, N.H., 2013, **Nondestructive Testing to Identify Delaminations Between HMA Layers Volume 1**, Strategic Highway Research Program (SHRP 2) report, Transportation Research Board, Washington D.C.

[27] Willis, J.R. and D.H. Timm, “A *Forensic Investigation of Debonding in a Rich-Bottom Pavement*,” Transportation Research Record 2040, Transportation Research Board, 2007, pp. 107-114.

[28] Lemieux, M., R. Gagné, B. Bissonnette, and M. Lachemi. 2005. Behavior of Overlaid Reinforced Concrete Slab Panels Under Cyclic Loading— Effect of Interface Location and Overlay Thickness. *ACI Structural Journal*, Vol. 102, No. 3, pp. 454–461.

[29] Nazarian, S., and D. Yuan. *Evaluation and Improvement of Seismic Pavement Analyzer*. Research Project Report 7-2936. Center for Highway Materials Research, University of Texas at El Paso, 1997.

[30] Nazarian, S., K. H. Stokoe II, and W. R. Hudson. *Use of Spectral Analysis of Surface Waves Method for Determination of Moduli and Thicknesses of Pavement Systems*. In Transportation Research Record 930, National Research Council, Washington, D.C., 1983, pp. 38–45.

[31] Stokoe II, K. H., S. G. Wright, J. A. Bay, and J. M. Roesset. *Characterization of Geotechnical Sites by SASW Method*. In *Geotechnical Characterization of Sites* (R. D. Woods, ed.), Oxford and IBH Publishing, New Delhi, India, 1994, pp. 15–26.

[32] Nazarian, S., M. R. Baker, and K. Crain. SHRP Report H-375: *Development and Testing of a Seismic Pavement Analyzer*. SHRP, National Research Council, Washington, D.C., 1993.

[33] Celaya, M., Nazarian, S., 2007, “Stripping Detection in Asphalt Pavements with Seismic Methods” *Transportation Research Record*, No. 2005, pp 64-74.

[34] McDaniel, M., Celaya, M., Nazarian, S., 2010, “Concrete Bridge Deck Quality Mapping with Seismic Methods-Case Study in Texas” *Transportation Research Record*, No. 2202, pp 53-60.

[35] Celaya, M., Nazarian, S., 2006, “Seismic Testing to Determine Quality of Hot-Mix Asphalt” *Transportation Research Record*, No. 1946, pp 113-122.

[36] Jurado, M., Gibson, N., Celaya, M., Nazarian, S., 2012, “Evaluation of Asphalt Damage and Cracking Development with Seismic Pavement Analyzer” *Transportation Research Record*, No. 2304, pp 47-54.

[37] Nazarian, S., Alvarado, G., 2006, “Impact of Temperature Gradient on Modulus of Asphaltic Concrete Layers” *JOURNAL OF MATERIALS IN CIVIL ENGINEERING* © ASCE, Vol. 18, No. 4, pp: 492-499.

[38] Baker, M. R., K. Crain, and S. Nazarian. Determination of Pavement Thickness with a New Ultrasonic Device. Research Report 1966-1. *Center for Highway Materials Research, University of Texas*, El Paso, 1995.

[39] National Bridge Inventory. FHWA, U.S. Department of Transportation, Dec. 2007. www.fhwa.dot.gov/bridge/defbr07.cfm.